Invited paper

OPTO-ELECTRONICS REVIEW **8**(3), 241–250 (2000)

Asymmetric multiple quantum well heterostructure laser systems: conception, performance, and characteristics

V.K. KONONENKO[1*], A.A. AFONENKO[2], I.S. MANAK[2], and S.V. NALIVKO[2]

[1]Stepanov Institute of Physics, National Academy of Sciences of Belarus,
70 Fr. Scorina Pr., 220072 Minsk, Belarus
[2]Belarussian State University, 4 Fr. Scorina Pr., 220050 Minsk, Belarus

A new type of laser diodes and amplifiers based on asymmetric quantum-well heterostructures having active layers of different thickness and/or compositions has been considered. Bistable switching and regimes of regular radiation pulsation at two or three remote wavelengths in the range 790–850 nm in the GaAs-AlGaAs bi- and triple-quantum-well heterostructures are described. Influence of non-linear processes including gain suppression due to carrier heating on lasing regimes has been examined. Transformation of gain bands for TE and TM modes in dependence on the pump current has been studied for asymmetric four-quantum-well structures. The interval of tuning amplification wavelengths in the system reaches up to 70 nm.

Keywords: quantum-well laser diodes, non-linear effects, bistability, regular pulsation, gain spectra.

1. Introduction

Multifunctional optical sources, e.g., multi-wavelength laser diodes have wide potential applications, such as light communications and information processing systems. Several technology solutions to attain lasing at two wavelengths and for a wide-range tuning have been already offered [1–4].

Use of asymmetric quantum-well (QW) heterostructures is a new conception of band engineering for semiconductor optoelectronics. Initial conception of the asymmetric multiple-QW heterostructure lasers was described early in 1991 [5–7]. Earlier, an asymmetric bi-QW laser diode with wavelength switching has been demonstrated [2,8]. Independently, strained multiple-QW lasers with designed varied QW width for control of the gain spectrum were suggested [9,10].

In sources based on asymmetric QW heterostructures it is possible to achieve the following behaviour and regimes: simultaneous CW lasing at two wavelengths [2,6–8], regular pulsation at two remote wavelengths [11,12], bistable power switching [13,14], regular pulsation at three remote wavelengths [15], extended gain spectrum [9], negative differential resistance effect [16], and polarisation insensitive gain [10]. New possibilities of controlling the optical and dynamic characteristics by widths, compositions, arrangement and order of the QWs, by cladding and barrier layer profile, introducing composite barriers, and using suitable barrier layer doping appear in QW heterostructure laser diodes. It gives opportunity to produce novel functional devices such as bistable logical elements [17], clock-pulse generators [18], multi-wavelength optical sources [5].

Application of QWs with varying widths and compositions gives additional degrees of freedom to stipulate required laser regimes. Asymmetric multiple-QW heterostructures are also used to study the carrier distribution across the active region of the lasers and to examine dependence of the carrier relaxation and transport processes on the QW parameters and laser structure design [19–21].

In the paper, a general description of opto-electronic properties of asymmetric QW heterostructure lasers is presented. Different possible regimes of operation and feature of laser response are described in detail.

2. Band diagram and current injection

The general equation system for calculation of electrophysical parameters of QW heterostructures includes Poisson's and the current continuity equations. The equation for the electrostatic potential φ is of the form

$$-\frac{d^2\varphi}{dz^2} = \frac{e}{\varepsilon\varepsilon_0}(p - n + N_d - N_a), \qquad (1)$$

where z is the co-ordinate along the axis normal to the plane of QW layers, n and p are the electron and hole concentrations, N_a and N_d are the concentrations of ionised acceptors and donors, ε is the dielectric constant. The energies E_c and E_v of the band edges depend on the potential φ as

*e-mail: lavik@dragon.bas-net.by

$$E_c = E_c(x) - e\varphi + C,$$
$$E_v = E_v(x) - e\varphi + C. \tag{2}$$

The choice of the constant C is arbitrary. In the GaAs-$Al_xGa_{1-x}As$ system, the energy profile of the conduction and valence bands, depending on the Al mole fraction x, can be determined in a linear approximation, i.e.,

$$E_c(x) = 1.424 + 0.848x \text{ (eV)},$$
$$E_v(x) = -0.399x \text{ (eV)}. \tag{3}$$

The continuity equations for the electron j_e and the hole j_h current densities at the assumption of quasi-equilibrium in the bands are of the form

$$\frac{dj_e}{dz} = eR, \quad j_e = \mu_e n \frac{dF_e}{dz}, \tag{4}$$

$$\frac{dj_h}{dz} = -eR, \quad j_h = \mu_h p \frac{dF_h}{dz}, \tag{5}$$

where R is the recombination rate, F_e and F_h are the quasi-Fermi levels, μ_e and μ_h are the mobilities of electrons and holes, respectively.

If excitation conditions of adjacent QWs i and k in a multiple-layer heterostructure are different, the electron (or hole) quasi-Fermi level can change in a barrier layer between the QWs significantly and carrier transport in the active region needs special consideration. Typically, barrier layer thickness does not exceed 50 nm and it is comparable with the mean free path of current carriers. Therefore ballistic transport of carriers through the barriers has a dominant role [22].

In the case of pure ballistic transfer, e.g., in the conduction band, the electron flow over a barrier between QWs arises in consequence of an imbalance of high-energy electrons at opposite sides of the barrier. Therefore in approach of the thermionic-emission theory one can write

$$j_b = e\bar{v}N_{cm}\left[\exp\left(\frac{F_{ek} - E_{cm}}{kT}\right) - \exp\left(\frac{F_{ei} - E_{cm}}{kT}\right)\right](1 + \gamma_e). \tag{6}$$

Here, $\bar{v} = \sqrt{kT/2\pi m_c}$ is the averaged carrier thermal velocity projection, m_c is the effective mass of electrons, E_{cm} is the maximum value of the conduction band edge energy in the barrier, N_{cm} is the effective density of states in the central part of the barrier, F_{ei} and F_{ek} are the quasi-Fermi levels at the sides of the barrier, T is the temperature, and the factor γ_e includes a contribution of tunneling [22].

A similar dependence of the current over a barrier on the quasi-Fermi levels can be also derived from general Eq. (4) under assumption of continuous F_e. Since recombination in the region of wide-band gap layer is negligible, Eq. (4) can be integrated in the z-co-ordinate interval from z_i to z_k, i.e.,

$$j_b = kT\mu_{eb}b_e\left[\exp\left(\frac{F_{ek}}{kT}\right) - \exp\left(\frac{F_{ei}}{kT}\right)\right]. \tag{7}$$

Here $b_e^{-1} = \int N_c^{-1}\exp(E_c/kT)dz$, where the effective density of states in the barrier N_c and the energy band edge E_c change in the z-direction from z_i to z_k. For the barrier currents according Eqs. (6) and (7) to be equal, we introduce an effective value of the electron mobility in the barrier region μ_{eb} which is determined by numerical solving Eqs. (1), (4), (5), and (7) in a self-consistent manner. The value μ_{eb} weakly depends on forward bias applied to the laser structure because variations in the charge distribution and the band edge profile $E_c(z)$ are small as a rule.

For further analysis it is useful to express the barrier current density j_b in terms of variables determining the excitation level of QWs. As calculations demonstrate, under high excitation of QWs that is needed for lasing, the quasi-Fermi level for holes (i.e., in the band opposite to the band with a potential barrier) in the region between the QWs is practically constant. At the central part of the barrier the relative position of the valence band top and the quasi-Fermi level for holes is invariable with respect to a change in pump current and it is determined by the barrier layer doping. Because of this, the change in the difference ΔF of the quasi-Fermi levels for electrons and holes in the barrier layer is due to the change in the position of the quasi-Fermi level for electrons. Then, an expression for the barrier current density at the carrier transport between adjacent QWs i and k has the form [23]

$$j_b = j_{b0}\left[\exp\left(\frac{\Delta F_k}{kT}\right) - \exp\left(\frac{\Delta F_i}{kT}\right)\right], \tag{8}$$

where ΔF_i and ΔF_k are the differences of the quasi-Fermi levels in QWs i and k. As seen, the barrier current depends on populations in the QWs and the carrier transfer occurs into the less excited QW. This is a main feature of current carrier transport in the barrier regions that has an effect on lasing dynamics.

The quantity j_{b0}, which serves as a characteristic parameter of the structure, is regulated by the change of the band gap, thickness, and doping of the barrier layer. If the carrier distribution in QWs is non-degenerate, $\exp(\Delta F/kT) \sim np \approx n^2$. At lasing excitation conditions, the dependence of the barrier current on the carrier concentrations in QWs is more strong than n^2 and assumes an exponential character. Note, that the rigorous functional dependence of the barrier current on the carrier concentrations has a minor importance for the describing of the laser response and impacts on obtained results only quantitatively.

3. Rate equations

Lasing in asymmetric QW heterostructures can be realised at several wavelengths λ_j. Introducing the photon densities at these wavelengths S_j and the sheet concentrations of minority charge carriers in QWs n_i we can write the following rate equations

$$\frac{dn_i}{dt} = \frac{j_i}{e} - R_i - \sum_j vG_i(\lambda_j)S_j, \tag{9}$$

$$\frac{dS_j}{dt} = \sum_i vG_i(\lambda_j)S_j - vK_lS_j + \sum_i \beta_{ij}R_i. \tag{10}$$

Here, t is the time, j_i is the current density of injection into QW i, R_i is the spontaneous recombination rate in QW i. If the leakage to the cladding and emitter layers is negligible, then $\Sigma j_i = j$, where j is the pump current density. A contribution of spontaneous emission to laser modes is given by multipliers $\beta_{ij} \approx 10^{-4}$.

The terms describing the stimulated emission recombination involve the modal gain coefficients $G_i(\lambda_j)$ represented by the products $\Gamma_i k_i(\lambda_j)$. The function $k_i(\lambda)$ describes the radiation gain spectrum in QW layer i. The optical confinement factor Γ_i defines a portion of the radiation at the wavelength λ_j propagating in QW i. Optical losses concerned with the output radiation from the cavity are given by the coefficient K_l. The light velocity in the crystal is denoted by v. If the photon energy $\hbar\omega_j = hc/\lambda_j$ is less than the energy gap between the lowest subband levels $E_{gi} = E_{c0} - E_{v0} + E_{c1} + E_{v1}$ in QW i, then, practically, $G_i(\lambda_j) \approx 0$ and $\beta_{ij} \approx 0$. Here, E_{c0} and E_{v0} are the bottom of the conduction band and top of the valence band, E_{c1} and E_{v1} are the ground subband energies in the conduction and valence bands. Notice, that, as distinct from the usual rate equations [24], in Eqs. (9) and (10) the photon density values in modes are reduced to the unit area in the plane of QW layers. Correspondingly, the radiative recombination rates are also presented per unit area.

4. Nonlinear gain effects

Gain non-linearity plays an important role in determining the modulation of output power and other aspects of laser diode response as well [25,26]. Usually, gain saturation is included in the rate equations by reducing the gain coefficient, e.g.,

$$G(\lambda,S) = \frac{G(\lambda,0)}{1+\varepsilon S} \approx G(\lambda,0)(1-\varepsilon S), \tag{11}$$

where ε is the phenomenological saturation factor. When stimulated radiation at several wavelengths is excited, simplified Eq. (11) describes only a non-linear gain due to spectral hole burning because radiation at definite wavelength does not modify the gain for another wavelengths.

Recent time much attention is paid to the carrier heating effects which are expected to provide a dominant contribution to the non-linear gain [27]. In the framework of the one-wavelength theory [28,29], the extension of Eqs. (9) and (10) to incorporate the non-linear gain can be made in the generalised form. In this case we have

$$\frac{dn_i}{dt} = \frac{j_i}{e} - R_i - \sum_j v[G_i(\lambda_j) - \sum_{j'} \varepsilon_{ijj'}G_i(\lambda_{j'})S_{j'}]S_j, \tag{12}$$

$$\frac{dS_j}{dt} = \sum_i v[G_i(\lambda_j) - \sum_{j'} \varepsilon_{ijj'}G_i(\lambda_{j'})S_{j'}]S_j - vK_lS_j + \sum_i \beta_{ij}R_i. \tag{13}$$

Here, $\varepsilon_{ijj'}$ are the nonlinear gain parameters introduced as follows

$$\varepsilon_{ijj'} = \frac{vG_{im}(\lambda_j)\tau_{eff}}{kT_eE_{LO}n_{int}}\left[\frac{\partial U_{ei}}{\partial n_i} - E_{csti}(\lambda_j)\right] \times\left[\frac{\partial U_{ei}}{\partial n_i} - E_{csti}(\lambda_{j'})\right] f_e[E_{csti}(\lambda_j)] \times\left\{1 - f_e[E_{csti}(\lambda_j)]\right\}, \tag{14}$$

where $G_{im}(\lambda_j)$ is the maximum modal gain, T_e is the electron temperature, E_{LO} is the optical phonon energy, $n_{int} = m_cE_{LO}/\pi\hbar^2$ is the effective concentration of electrons which interact with the phonons, U_{ei} is the energy of electron subsystem in QW i, $f_e(E_{csti})$ is the electron distribution function, $E_{csti}(\lambda_j) = E_{c0} + E_{c1} + (\hbar\omega_j - E'_{gi})/(1 + m_c/m_v)$ is the electron energy at direct transitions, m_c and m_v are the effective masses of electrons and holes. The effective relaxation time τ_{eff} takes into account degeneracy and hot-phonon effects and equals

$$\tau_{eff} = \frac{1}{n_{LO}(n_{LO}+1)} \times\left(\tau_{el-ph} + \Gamma_{ph}\tau_{ph}\frac{n_{int}}{n_{ph}}\right)\frac{kT_e}{E_{LO}}, \tag{15}$$

where n_{LO} is the Bose-Einstein occupation number at the phonon temperature $T_{ph} = T_e$, τ_{el-ph} is the scattering time constant for the process, Γ_{ph} is a phonon confinement factor, τ_{ph} is the phonon lifetime, $n_{ph} \approx 2n$ is the density of the phonon modes most strongly interacting with electrons.

Estimations of the non-linear gain parameter at room temperature have been performed for a QW with width d = 10 nm, $\Gamma = 0.025$, $G_m = 150$ cm^{-1}, $\Gamma_{ph} = 1$, and constants $\tau_{el-ph} = 368$ fs, $\tau_{ph} = 4$ ps, $E_{LO} = 34$ meV, $m_c = 0.07\ m_e$ [29]. Results of calculations of the non-linear gain parameter at the wavelength λ_j when the non-linearity

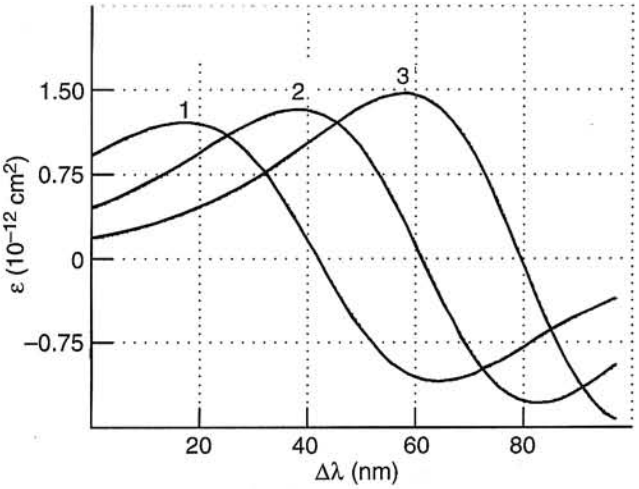

Fig. 1. The nonlinear gain parameter ε at the wavelength λ versus the mismatch $\Delta\lambda = \lambda' - \lambda$, where λ′ corresponds to the transitions between ground energy levels in the QW. (1) $n = 2\times10^{12}$ cm^{-2}, $\tau_{eff} = 2.0$ ps, (2) $n = 3\times10^{12}$ cm^{-2}, $\tau_{eff} = 1.5$ ps, (3) $n = 4\times10^{12}$ cm^{-2}, $\tau_{eff} = 1.3$ ps.

is induced by radiation at the wavelength λ_j, corresponding to the transitions between the lowest energy levels in the QW are presented in Fig. 1. If $E_{cst}(\lambda_j)$ does not exceed $\partial U_e / \partial n$, then $\varepsilon \approx 10^{-12}$ cm^2 that corresponds to the analogous bulk parameter $\varepsilon_V = \varepsilon d/\Gamma \approx 4\times10^{-17}$ cm^3. In the calculations below we neglect the non-linear gain dispersion and use $\varepsilon_{ijj} \equiv \varepsilon$. Account of the dispersion of the non-linear gain is essential for detail explanation of the observed dynamic and static response of asymmetric QW heterostructure lasers [24].

5. Bistable switching

Analysis of Eqs. (12) and (13), as applied to the asymmetric bi-QW (ABQW) heterostructure with the band diagram on Fig. 2, shows a possibility of realising the bistable output radiation regime. Here, the QW at the p-type emitter is denoted as 1, the QW at the n-type emitter is denoted as 2. The QW layers in the GaAs-$Al_xGa_{1-x}As$ system have the same band gap widths (x = 0) and different thickness (d_1 = 8 nm, d_2 = 10 nm). The regime of bistable switching takes place if the excited oscillation mode is absorbed in one QW [13]. Therefore the structure is formed in such a way that the barrier layer between QWs is doped with donors. The potential barrier arising in the valence band partly blocks the hole transport into QW 2 and inhomogeneous excitation of the active region is put into effect. Then, the lasing mode at λ_1 = 831 nm, which corresponds to transitions between ground levels in QW 1, is amplified in this QW and absorbed in QW 2.

The dependence of the injection current on QW populations is a specific feature of ABQW heterostructures in compare to ordinary bistable lasers where gain and absorption sections work separately. Such dependence is unwanted because it prevents the fulfilment of the conditions

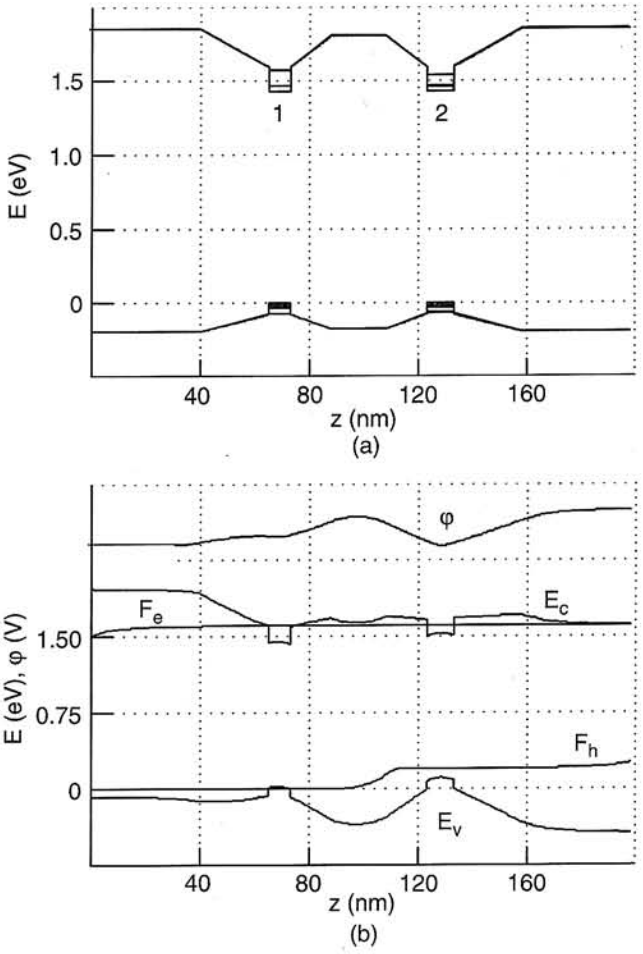

Fig. 2. Configuration of the band gap energy E(z) and the subband levels of an ABQW structure in the GaAs-$Al_xGa_{1-x}As$ system (a) and the ABQW heterostructure band diagram at the forward bias of 1.6 V (b).

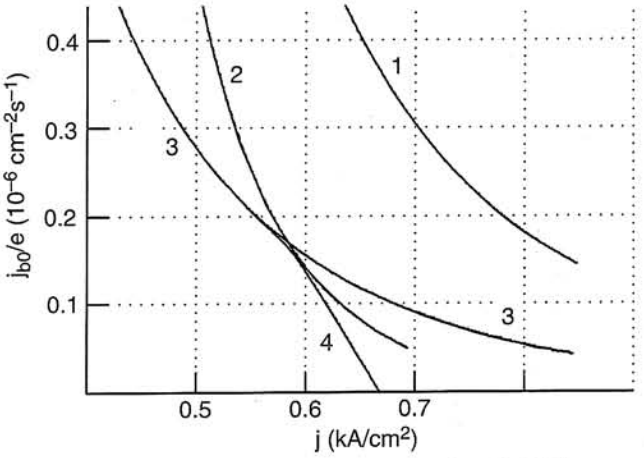

Fig. 3. Boundaries of different regimes for the ABQW laser at $K_l = 40$ cm^{-1} in accordance with the injection current density j and parameter j_{b0}: (1) curve of zero-absorption at the wavelength λ_1 in QW 2, (2) threshold curve for switch-on operation, (3) bound of hard switching regime, (4) threshold curve for switch-off operation.

of "hard" switching-on [30]. The elimination of the effect can be reached by reduction of the barrier current density j_b. For absorption of the λ_1 mode in QW 2 not to be very high to inhibit lasing, the energy band gap between the ground levels in this QW is chosen to be close to the photon energy of stimulated emission.

The theoretical regions of different lasing regimes of the ABQW structure in the j–j_{b0} space are shown in Fig. 3. In the region below curve 1 QW 2 serves as an absorber at λ_1. Curve 2 corresponds to the lasing threshold at λ_1. Below bound 3 the total gain $G_1(\lambda_1)+G_2(\lambda_1)$ has a maximum versus the photon density S_1. From the point of intersection of threshold curve 2 and bound 3 curve 4 appears along which the maximum total gain equals the losses K_1. The difference between curves 2 and 4 at a constant j_{b0} determines a hysteresis of the power-current characteristic.

Increase in pump current leads to the jump-like appearance of output radiation after exceeding the threshold current (Fig. 4). It is accompanied by a step-like changing in carrier concentrations in the QWs. The radiation flow causes the population in QW 2 to grow. The absorption of the lasing mode in QW 2 saturates and the gain in QW 1 drops. Therefore the population in QW 1 decreases. The switch-off of lasing at reduction of the pump current occurs at a current value that is smaller than the threshold current. This scheme for obtaining the optical bistability can be classified as a "parallel" scheme.

6. Pulse generation at two wavelengths

Another ABQW heterostructure band diagram in the GaAs-$Al_xGa_{1-x}As$ system is shown in Fig. 5. Here, QW 1 lasing at the wavelength λ_1 is positioned at the p-type emitter side, and QW 2 is positioned at the n-type emitter side and radiates at the wavelength λ_2. For λ_1 and λ_2 to be different, QW layers with the same thickness ($d_1 = d_2 = 10$ nm) have different band gap semiconductors ($x_1 = 0$, $x_2 = 0.07$). For such ABQW heterostructures the wide-band gap barrier layer separating QWs can be with a linear or parabolic potential energy profile, as in conventional laser heterostructures with a separate confinement and graded index. The potential form and dimensions of the barrier layer have been chosen in such a way that holes easily pass into

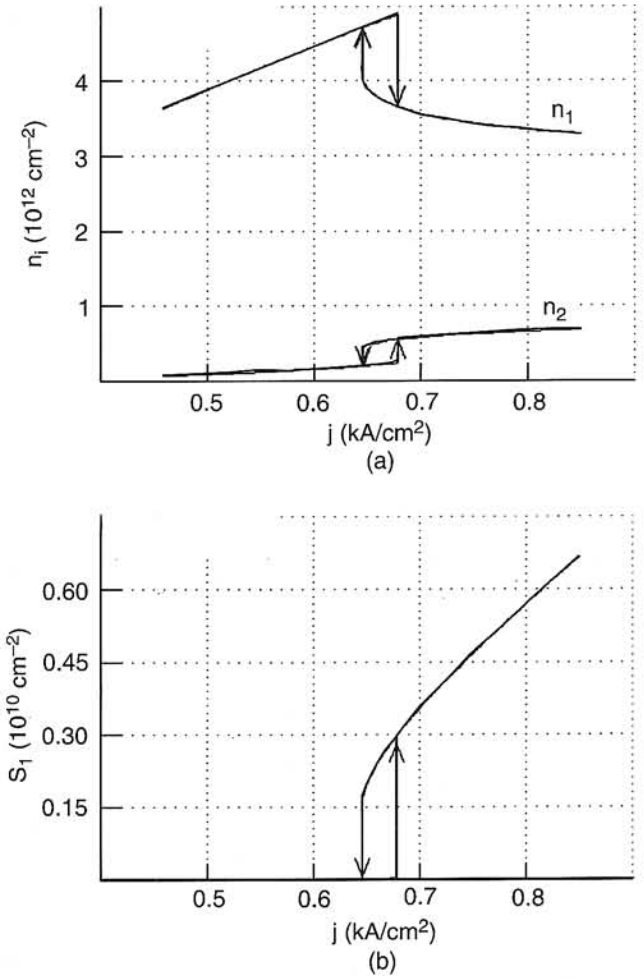

Fig. 4. Change in carrier concentrations n_i in different QWs (i = 1,2) (a) and power switching at the single lasing mode S_1 with a hysteresis loop behaviour at $j_{b0}/e = 5\times10^{-8}$ cm^{-2}s^{-1} (b).

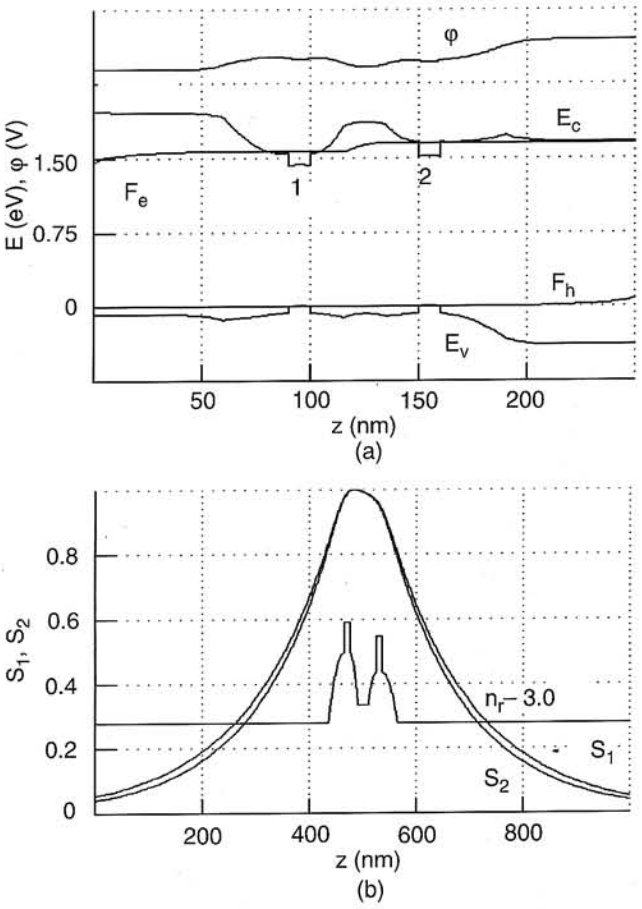

Fig. 5. Band diagram of an ABQW laser structure at the forward bias of 1.65 V (a); spatial normalised distributions of laser mode intensities S_1 and S_2 at the wavelengths λ_1 = 844 nm and λ_2 = 802 nm and the refractive index profile $n_r(z)$ in the structure waveguide region (b).

QW 2 but the electron transfer into QW 1 is more difficult. The efficiency of the carrier injection into QW 1 can be arbitrary changed through the choice of the barrier layer band gap and its doping. Doping with acceptors encourages the origin of a potential barrier for electrons. Using Eq. (8) we derive the efficiency of current injection into the QWs as $\eta_1 = j_1/j = j_b/j$ and $\eta_2 = j_2/j = 1-\eta_1$.

Theoretical regions of the existence of different oscillation modes in the space $j-j_{b0}$ are shown in Fig. 6. In region I, stationary lasing is achieved only at the wavelength λ_1. If the threshold at the wavelength λ_1 is not reached, the laser emits regular radiation pulses at another mode at the wavelength λ_2 (region II). Simultaneous excitation of both laser modes occurs in region III. The regions enclosed by dashed lines identify ranges of the parameters where self-sustained pulsation at the both wavelengths exist at different values of the gain suppression factor ε. The threshold curve between regions II and III has a pure conditional character in the instability range as it was determined in the small-signal approach.

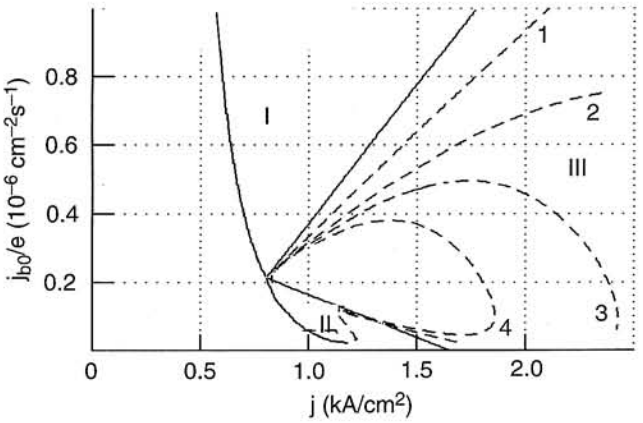

Fig. 6. Regions of excitation of different oscillation modes for the ABQW laser at $K_l = 40$ cm^{-1} in accordance with the injection current density j and parameter j_{b0}. (I) lasing at the wavelength $\lambda_1 = 844$ nm, (II) lasing at the wavelength $\lambda_2 = 802$ nm, (III) simultaneous oscillations at two wavelengths. The dashed lines show boundaries of the regions of the existence of pulsation at the suppression factor ε equal to (1) 0, (2) 2×10^{-12}, (3) 3×10^{-12}, and (4) 4×10^{-12} cm^2. The boundaries between regions I–III and II–III have been calculated at $\varepsilon = 0$.

The main cause of appearance of the unstable lasing is associated with the presence of absorption of the radiation at the shorter wavelength in the QW emitting at the longer wavelength. It is proved by the analysis of Eqs. (9) and (10) at assumption of constant injection efficiencies [12]. However, the presence of injection coupling between the QWs essentially determines nature of self-sustained radiation pulsation.

Results of simulation of the lasing dynamics of ABQW structures are presented in Fig. 7. When simultaneous lasing at two modes occurs, the absorption of the more intensive λ_2 mode in QW 1 competes with the process of population reset as a consequence of lasing at the λ_1 mode. Increasing population in one of the QWs causes a decrease in the efficiency of injection into this QW and increases the carrier injection into another QW. As a result, the process of radiation pulsation is accompanied by oscillations of the efficiencies of carrier injection into the QWs. Thus, owing

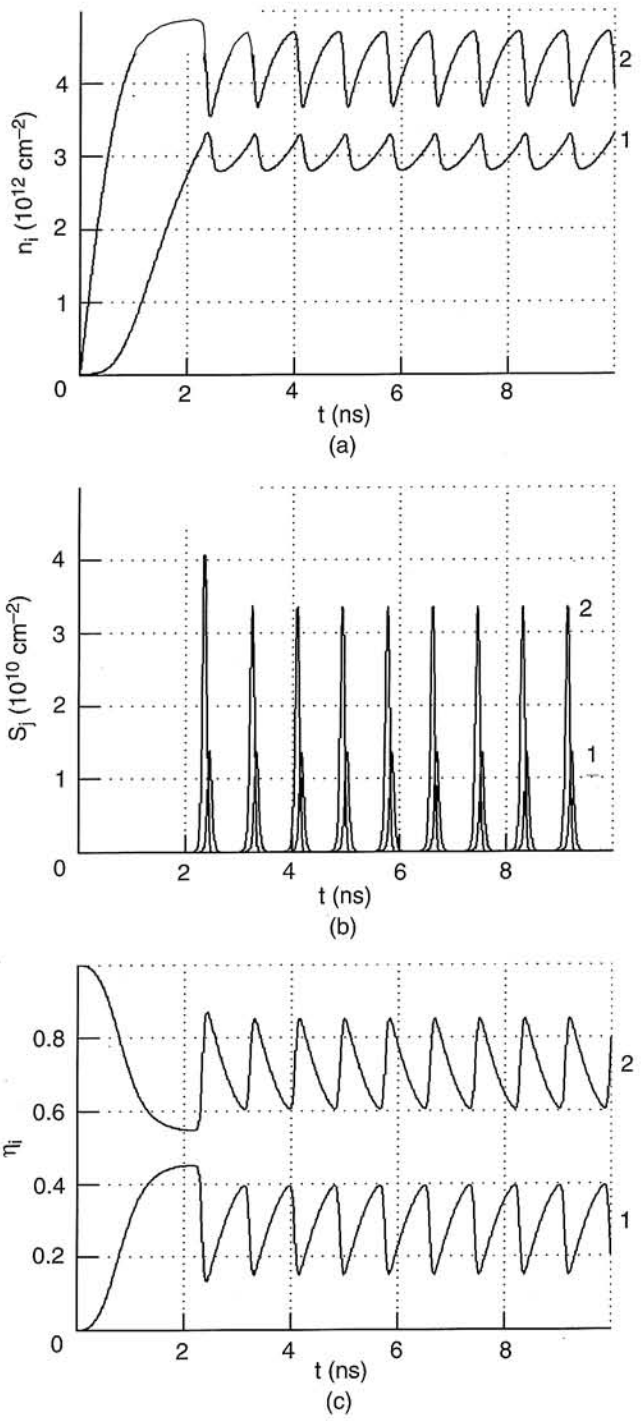

Fig. 7. Oscillations of the electron concentrations n_i in different QWs (i = 1,2) (a), radiation pulsation at two separated wavelengths λ_j (j = 1,2) (b), and oscillations of the injection efficiencies η_i (i = 1,2) at $K_l = 40$ cm^{-1}, j = 1.1 kA/cm^2, $j_{b0}/e = 0.3\times10^{-6}$ cm^{-2}s^{-1}, $\varepsilon = 2\times10^{-12}$ cm^2 (c).

to the nonlinear electron-optical interaction of QWs in ABQW structures a synchronization effect arises [30] and radiation pulses at different wavelengths follow one another. The effect of gain suppression leads to a contraction of the region of pulsation, radiation pulses become smaller in amplitude and longer in duration.

Simulation of the lasing dynamics shows that, depending on configuration of ABQW heterostructures, the duration of the light spikes can be varied in the range of 50 to 250 ps. The relative delay between the sequential light pulses at two remote λ_1 and λ_2 modes is about 10% of the pulsation period which can be controlled in a wide range by the pump current.

7. Regular pulsation at three wavelengths

A profile of the band gap of an asymmetric triple-QW (ATQW) heterostructure is shown in Fig. 8. To provide the emission of QWs at different wavelengths, the materials forming the QWs have different band gaps which are determined by the Al molar content $x_1 = 0$, $x_2 = 0.04$, and $x_3 = 0.065$. To produce nearly equal levels of injection into different QWs, between them there are compound barrier layers doped with acceptors.

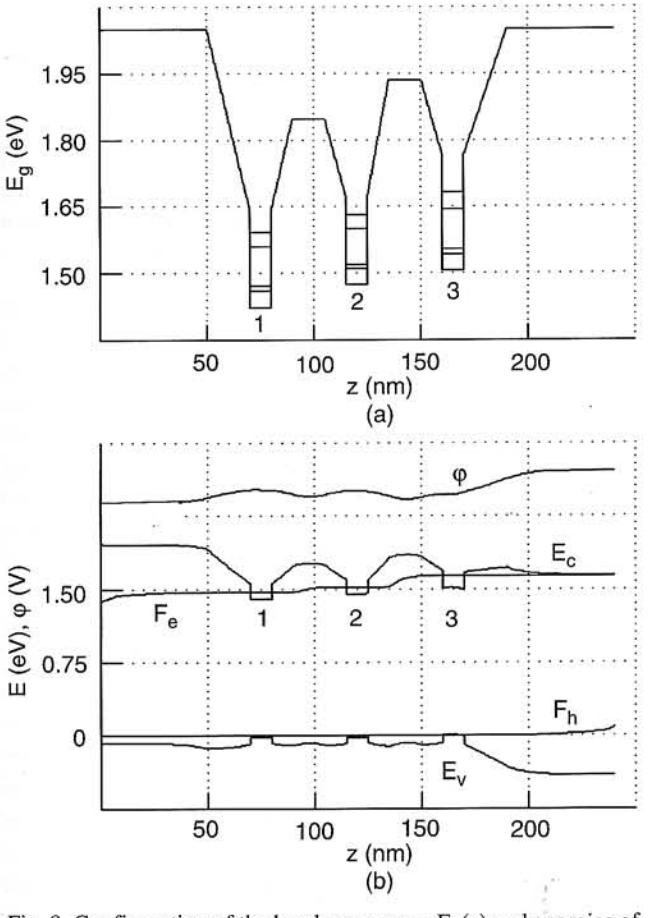

Fig. 8. Configuration of the band gap energy $E_g(z)$ and energies of optical transitions for an ATQW structure in the GaAs-$Al_xGa_{1-x}As$ system (a) and band diagram of the structure at the forward bias of 1.63 V (b).

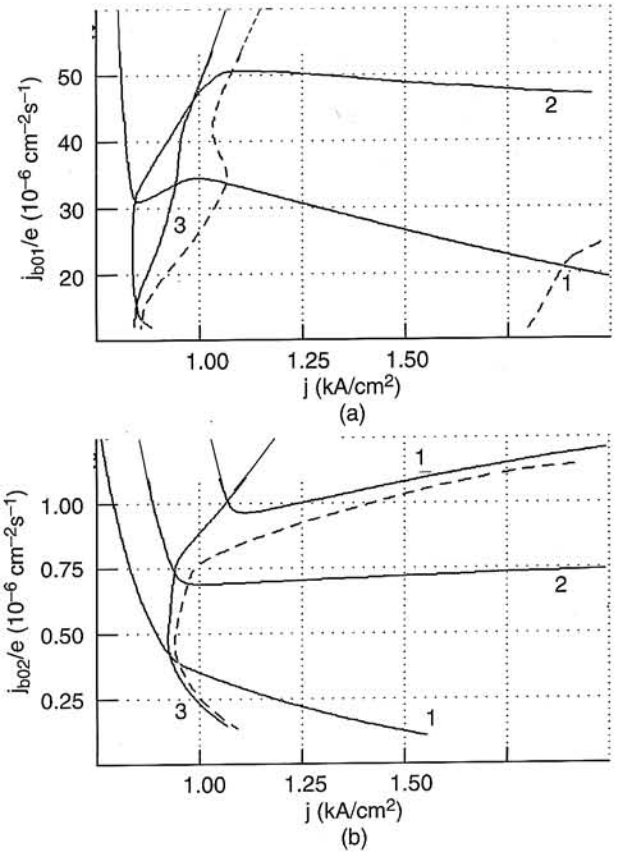

Fig. 9. Regions of excitation of different oscillation modes of the ATQW laser at $K_l = 40$ cm^{-1} in accordance with the current density j and parameters (a) j_{b01} at $j_{b02}/e = 8\times10^{-7}$ $cm^{-2}s^{-1}$ and (b) j_{b02} at $j_{b01}/e = 4\times10^{-5}$ $cm^{-2}s^{-1}$. (1) threshold at the wavelength $\lambda_1 = 842$ nm, (2) threshold at the wavelength $\lambda_2 = 821$ nm, (3) threshold at the wavelength $\lambda_3 = 804$ nm. The dashed lines show boundaries of the stable lasing regions at the suppression factor $\varepsilon = 2\times10^{-12}$ cm^2.

As for the structure shown in Fig. 8, potential barriers lead to the blocking of the electron transfer and do not keep holes from transport to QWs 2 and 3. Excitation level of QW 3 having the largest band gap is determined by applied voltage. A laser ATQW structure with potential barriers between QWs in different energy bands can be also designed [14]. Using Eq. (8), we find current densities of injection into the QWs $j_1 = j_{b1}$, $j_2 = j_{b2} - j_{b1}$, and $j_3 = j - j_{b2}$. It is necessary, therewith, to use two independent parameters j_{b01} and j_{b02}, according to the number of barriers in this structure.

Lasing in the structure under consideration is performed at three wavelengths $\lambda_1 = 842$ nm, $\lambda_2 = 821$ nm, and $\lambda_3 = 804$ nm. Theoretical regions of the existence of different oscillation modes in the spaces $j-j_{b01}$ and $j-j_{b02}$ when $\varepsilon = 2\times10^{-12}$ cm^2 are shown in Fig. 9. Threshold curves for corresponding wavelengths are denoted by figures. The dashed lines mark boundaries of stable lasing. Results of simulation of the dynamic response of the ATQW structure described above are presented in Fig. 10. Light spikes at different wavelengths follow one another, the first spike in the consequence is the mode at the shortest wavelength, and the last spike is the mode at the longest wavelength.

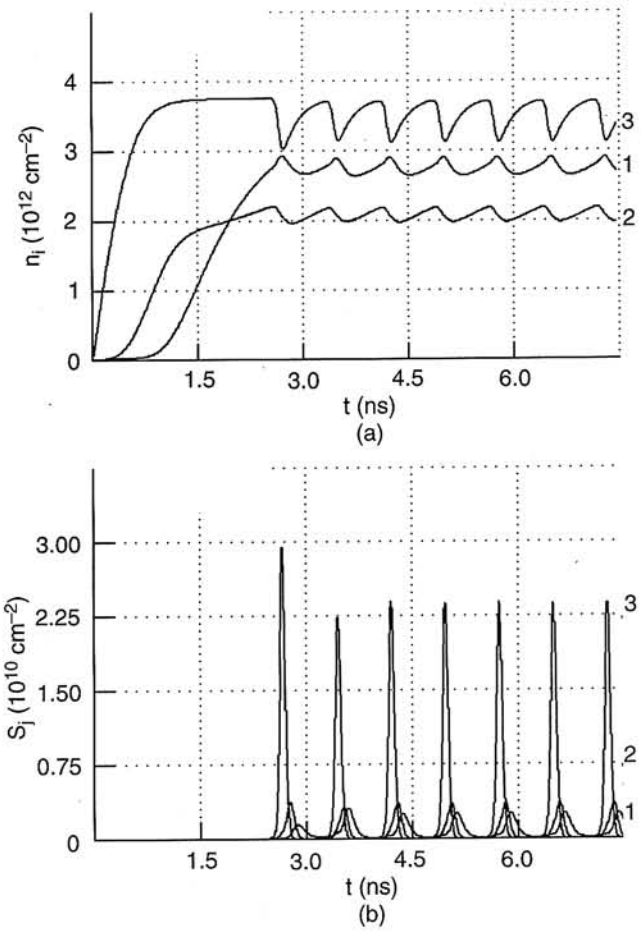

Fig. 10. Oscillations of the electron concentrations n_i in different QWs (i = 1,2,3) (a) and lasing pulses at three remote wavelengths λ_j (j = 1,2,3) at $K_1 = 40$ cm^{-1}, j = 1.1 kA/cm^2, $j_{b01}/e = 4\times10^{-5}$ cm^{-2}s^{-1}, $j_{b02}/e = 8\times10^{-7}$ cm^{-2}s^{-1}, $\varepsilon = 2\times10^{-12}$ cm^2 (b).

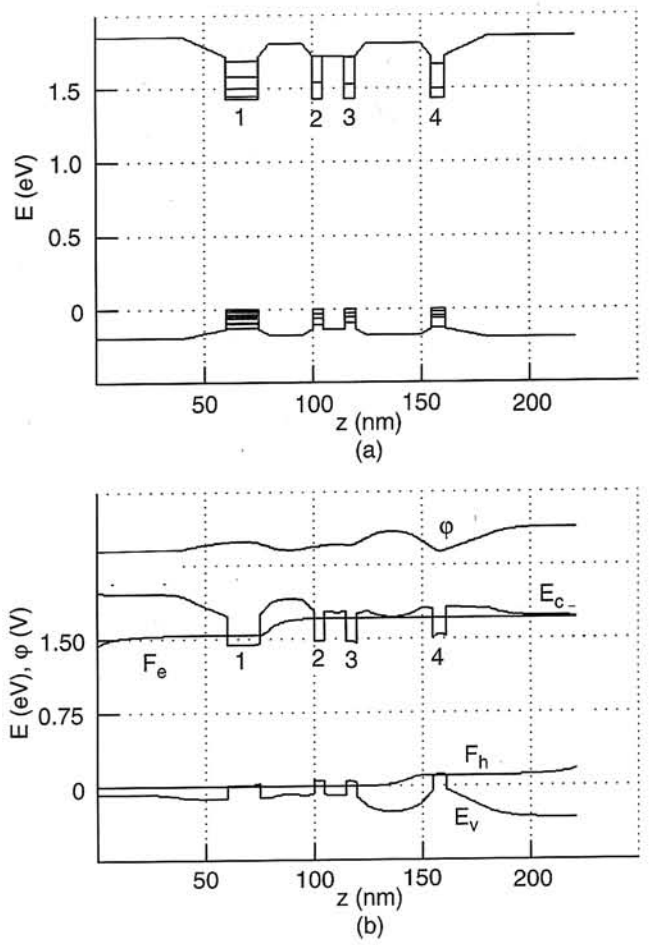

Fig. 11. Configuration of the band gap of an asymmetric heterostructure with four QWs, the subband levels for electrons and holes are shown (a); band diagram of the structure at the forward bias of 1.71 V, j = 1.9 kA/cm^2 (b).

8. Extended gain spectra

The continuously tunable from 766 to 856 nm laser diode in a grating coupled ring cavity was demonstrated using an asymmetric bi-QW heterostructure [31]. The similar laser structure was used to achieve simultraneous tuning at two wavelenghts [32]. The tuning range of 911 to 981 nm was obtained for a laser diode with three QWs of different widths in an external cavity of the Littrow configuration [33]. Design of tunable asymmetric QW laser diodes in the Littman and Metcalf cavity configuration is described as well [34].

Extended tunable gain spectra are easily realised in asymmetric multiple-QW (AMQW) heterostructures under the non-uniform excitation conditions. There are some design diagrams of the widely tunable AMQW heterostructure laser diodes [35–37]. The active region of the lasers can differ in thickness and component compositions of the QWs and barrier layers and in order of the QWs relative to each other and wide-band gap emitters. A design of such a structure in the GaAs-$Al_xGa_{1-x}As$ system is shown in Fig. 11.

The laser active region consists of four QWs with widths d_1 = 15 nm, d_2 = 4.5 nm, d_3 = 5.0 nm, and d_4 = 6.5 nm. Calculations of the gain spectra have been performed in a model of radiative transitions with the **k**-selection rule. The spectral radiation line broadening due to finiteness of the intraband carrier relaxation time is taking into account [38]. A shape of the radiation line is described by the Lorentzian with the broadening parameter equal to 10 meV. The polarisation dependence of the optical transition probability is taking into account too [39,40].

The range of tuning the gain for this structure reaches up to 70 nm (Fig. 12). The widest QW amplifies the radiation at the long-wavelength region with the gain maximum at the wavelength $\lambda \approx 860$ nm. Narrow QWs 2 and 3 amplify radiation at the short-wavelength region at the wavelength $\lambda \approx 780$ nm. Since QW 1 gives an intense absorption in this region of the spectrum, two QWs with different widths are used for compensatien of the radiation losses. Excitation of QWs 2 and 3 is connected with the voltage applied to the structure. Excitation of QW 1 is controlled by the width, composition, and doping of the barrier layer between QWs 1 and 2. To achieve nearly flat gain profile there is QW 4 amplifying radiation in the central part of the

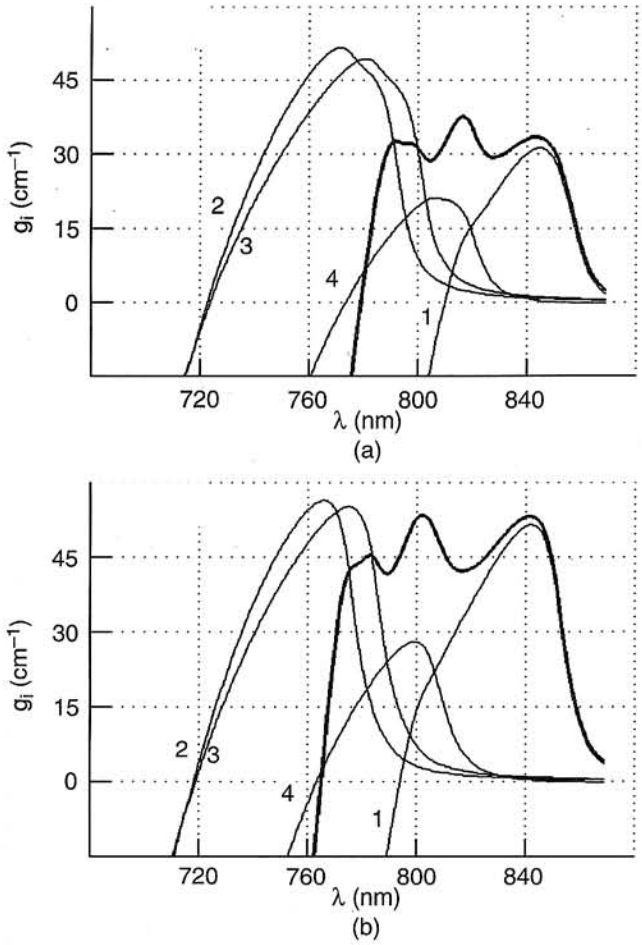

Fig. 12. The modal gain spectra $G_i(\lambda)$ of the asymmetric four-QW heterostructure: (a) for the TE mode at the pump current density j = 1.9 kA/cm^2 and (b) for the TM mode at j = 2.5 kA/cm^2. The solid curves refer to the total gain. Figures on the curves correspond to the QW numbers i = 1,..., 4.

spectrum. Thus, selecting the parameters of barriers and the injection current it is possible to control the modal gain in a wide spectral range. At increasing the excitation of the structure, the carrier injection will mainly grow into QWs 1 and 4. Absorption in these QWs significantly decreases and the maximum of the total gain is shifted in the short-wavelength region of the spectrum.

9. Conclusions

The simulation performed of asymmetric bi- or triple- QW laser heterostructures allows one to chose the active region parameters for required regimes of operation such as bistable switching and regular pulsation at two or three remote wavelengths. In accordance with the structure configuration and conditions of pumping, both the spectral and output power characteristics of these laser systems can be easily changed. Use of asymmetric QW heterostructures gives new opportunities to extend gain spectra and essentially to weaken its sensitivity to polarisation.

Acknowledgements

The work was financed under Grants of the Belarussian Republican Foundation for Fundamental Research and supported in part by the International Soros Science Education Program.

References

1. Y. Tokuda, Y. Abe, T. Matsui, N. Tsukada, and T. Nakayama, "Dual-wavelength emission from a twin-stripe single quantum well laser," *Appl. Phys. Lett.* **51**, 1664–1666 (1987).
2. S. Ikeda, A. Shimizu, and T. Hara, "Asymmetric dual quantum well laser – wavelength switching controlled by injection current," *Appl. Phys. Lett.* **55**, 1155–1157 (1989).
3. S. Ikeda, A. Shimizu, Y. Sekiguchi, M. Hasegawa, K. Kaneko, and T. Hara, "Wide-range wavelength tuning of an asymmetric dual quantum well laser with inhomogeneous current injection," *Appl. Phys. Lett.* **55**, 2057–2059 (1989).
4. K.J. Beernink, R.L. Thornton, and H.F. Chung, "Low threshold current dual wavelenght planar burried heterostructure lasers with close spatial and large spectral separation," *Appl. Phys. Lett.* **64**, 1082–1084 (1994).
5. V.K. Kononenko and S.A. Lomashevich, "Semiconductor Light Amplifier," *Patent RU*, No. 2062543 (July 1991).
6. V.K. Kononenko, "Two-frequency quantum-well optical structure," in *Tech. Digest, Int. Topical Meeting on Photonic Switching*, p. 2J1, Minsk, 1992.
7. V.K. Kononenko, "Spectral characteristics of quantum-well heterolasers," *Proc. SPIE* **1724**, 89–101 (1992).
8. S. Ikeda and A. Shimizu, "Evidence of the wavelength switching caused by a blocked carrier transport in an asymmetric dual quantum well laser," *Appl. Phys. Lett.* **59**, 504–506 (1991).
9. D. Teng, Y.H. Lo, C.H. Lin, and L.F. Eastman, "Effects of nonuniform well width on compressively strained multiple quantum well lasers," *Appl. Phys. Lett.* **60**, 2729–2731 (1992).
10. A. Mathur and P.D. Dapkus, "Polarization insensitive strained quantum well gain medium for lasers and optical amplifiers," *Appl. Phys. Lett.* **61**, 2845–2847 (1992).
11. V.K. Kononenko, I.S. Manak, and A.A. Afonenko, "Radiation oscillation processes in quantum-well heterolasers," *Proc. SPIE* **2039**, 66–77 (1993).
12. A.A. Afonenko, V.K. Kononenko, and I.S. Manak, "Regime of regular pulsation in lasers with two quantum wells," *J. Tech. Phys. Lett.* **20**, 57–61 (1994).
13. A.A. Afonenko, V.K. Kononenko, and I.S. Manak, "Bistable regime of generation in quantum-well lasers," *J. Tech. Phys. Lett.* **19**, 35–39 (1993).
14. A.A. Afonenko, V.K. Kononenko, and I.S. Manak, "Bistable laser source," *Bull. Russ. Acad. Sci., Phys. Ser.* **58**, 70–73 (1994).
15. A.A. Afonenko, V.K. Kononenko, and I.S. Manak, "Current injection and recombination processes in asymmetric triple quantum-well lasers," *Proc. SPIE* **2399**, 329–334 (1995).
16. P.C. Mogensen, G. Kelly, J. Keel, P.A. Evans, P. Blood, and J.S. Roberts, "Negative differential resistance in GaAs-AlGaAs asymmetric double quantum well laser struc-

tures," in *Programme and Abstracts, Semiconductor and Integrated Optoelectronics Conference*, Cardiff, 1996.
17. V.K. Kononenko, A.A. Afonenko, and I.S. Manak, "Bistable Semiconductor Laser Element," *Patent BY*, No. 1099 (Dec. 1993).
18. A.A. Afonenko, V.K. Kononenko, and I.S. Manak, "Semiconductor Laser," *Patent BY*, No. 1385 (July 1994).
19. P.A. Evans, P. Blood, and J.S. Roberts, "Carrier distribution in quantum well lasers," *Semicond. Sci. Technol.* **9**, 1740–1743 (1994).
20. H. Hillmer and S. Marcinkevičius, "Optically detected carrier transport in III/V semiconductor QW structures: experiment, model calculations and applications in fast 1.55 μm laser devices," *Appl. Phys.* **B 66**, 1–17 (1998).
21. M.J. Hamp, D.T. Cassidy, B.J. Robinson, Q.C. Zhao, D.A. Thompson, and M. Davies, "Effect of barrier height on the uneven carrier distribution in asymmetric multiple-quantum-well InGaAsP lasers," *IEEE Photon. Technol. Lett.* **10**, 1380–1382 (1998).
22. M. Shur, *GaAs Devices and Circuits*, Chs. 2 and 11, Plenum Press, New York, 1987.
23. A.A. Afonenko, V.K. Kononenko, and I.S. Manak, *Modelling of Novel Light Sources Based on Asymmetric Heterostructures*, Laser, Atomic and Molecular Physics Ser. Report ICTP, LAMP/95/6, Trieste, 1995.
24. S. Ikeda and A. Shimizu, "Theoretical analysis of dynamic response of asymmetric dual quantum well lasers," *Appl. Phys. Lett.* **61**, 1016-1018 (1992).
25. C.Y. Tsai, C.Y. Tsai, Y.H. Lo, and R.M. Spencer, "Effects of spectral hole burning, carrier heating, and carrier transport on the small-signal modulation response of quantum well lasers," *Appl. Phys. Lett.* **67**, 3084–3086 (1995).
26. E.A. Avrutin, E.L. Portnoi, and A.V. Chelnokov, "Influence of nonlinear gain on Q-modulation regime characteristics in semiconductor lasers with rapid saturable absorber," *J. Tech. Phys. Lett.* **17**, 49–54 (1991).
27. B.N. Gomatam and A.P. DeFonzo, "Theory of hot carrier effects on nonlinear gain in GaAs-GaAlAs lasers and amplifiers," *IEEE J. Quantum Electron.* **26**, 1689–1704 (1990).
28. G. Wang, R. Nagarajan, D. Tauber, and J. Bowers, "Reduction of damping in high-speed semiconductor lasers," *IEEE Photon. Technol. Lett.* **5**, 642–645 (1993).
29. L.F. Lester and B.K. Ridley, "Hot carrier and frequency responce of quantum well lasers," *J. Appl. Phys.* **72**, 2579–2588 (1992).
30. V.K. Kononenko, A.A. Afonenko, and I.S. Manak, *Electron-Optical Nonlinear Interaction in Asymmetric Quantum-Well Laser Heterostructures*, Preprint ICTP, IC/94/284, Trieste, 1994.
31. B.L. Lee and C.F. Lin, "Wide-range tunable semiconductor lasers using asymmetric dual quantum wells," *IEEE Photon. Technol. Lett.* **10**, 322–324 (1998).
32. C.F. Lin, M.J. Chen, and B.L. Lee, "Wide-range tunable dual-wavelength semiconductor laser using asymmetric dual quantum wells," *IEEE Photon. Technol. Lett.* **10**, 1208–1210 (1998).
33. H.S. Gingrich, D.R. Chumney, S.Z. Sun, S.D. Hersee, L.F. Lester, and S.R.J. Brueck, "Broadly tunable external cavity laser diodes with staggered thickness multiple quantum wells," *IEEE Photon. Technol. Lett.* **9**, 155–157 (1997).
34. S.V. Nalivko, V.K. Kononenko, and I.S. Manak, "Design and characteristics of widely tunable quantum-well heterostructure lasers in the Littman and Metcalf cavity configuration," in *Proc. Int. Conf. on Transparent Optical Networks*, pp. 215–218, Kielce, 1999.
35. V.K. Kononenko, I.S. Manak, and S.V. Nalivko, "Design and characteristics of widely tunable quantum-well laser diodes," *Spectrochimica Acta* **A 55**, 2091–2096 (1999).
36. V.K. Kononenko, I.S. Manak, and S.V. Nalivko, "Characteristics of quantum-well heterostructures with broad-band controllable radiation," in *Proc. VIII Int. Symp. Advanced Display Technologies*, pp. 239–244, Novy Svit, 1999.
37. V.K. Kononenko, S.V. Nalivko, and I.S. Manak, "Quantum-well heterostructure laser diodes with flat widely tunable gain spectra," *Proc. SPIE* **3947**, 209–214 (2000).
38. M. Yamada, H. Ishiguro, and H. Nagato, "Estimation of the intra-band relaxation time in undoped AlGaAs injection laser," *Jpn. J. Appl. Phys.* **19**, 135–142 (1980).
39. V.K. Kononenko and S.V. Nalivko, "Spectral characteristics of asymmetric quantum-well heterostructure laser sources," *Proc. SPIE* **2693**, 760–767 (1996).
40. V.K. Kononenko, I.S. Manak, S.V. Nalivko, V.A. Shevtsov, and D.S. Shulyaev, "Gain and luminescence spectra of broadband emitters based on asymmetric quantum-well heterostructures," *J. Appl. Spectrosc.* **64**, 234–241 (1997).

